Letter

Holographic entropy inequalities and the topology of entanglement wedge nesting

Bartłomiej Czech, Sirui Shuai, Yixu Wang, and Daiming Zhang
Institute for Advanced Study, Tsinghua University, Beijing 100084, China

(Received 5 November 2023; accepted 5 March 2024; published 10 May 2024)

We prove two new infinite families of holographic entropy inequalities. A key tool is a graphical arrangement of terms of inequalities that is based on entanglement wedge nesting. It associates the inequalities with tessellations of the torus and the projective plane, which reflect a certain topological aspect of entanglement wedge nesting. The inequalities prove a prior conjecture about the holographic entropy cone. We discuss their relation to black hole physics and differential entropy, and sketch applications to quantum error correction, quantifying randomness of quantum states, and others.

DOI: 10.1103/PhysRevD.109.L101903

Introduction. Recent years have revealed the importance of classifying and studying quantum states according to their patterns of entanglement. One important class of quantum states are those whose entanglement entropies can be computed by a minimal cut prescription. The prescription assumes that the state can be represented by an auxiliary "bulk" structure, typically a tensor network or—in holographic duality [1]—a bulk geometry. The minimal cut prescription equates the entanglement entropy of a region X with the weight of a bulk cut, which separates X from $\bar{X}$ (the complement of X). The prescription is valid for all random tensor network states [2] at large bond dimension and—in holographic duality—for the dominant area term in the Ryu-Takayanagi proposal [3–6].

This paper concerns constraints on entanglement entropies, which are implied by the minimal cut prescription. Because of the application to holographic duality, such constraints are conventionally called "holographic entropy inequalities." In the vector space of hypothetical assignments of entropies to regions (entropy space), the locus of saturation of each holographic inequality is a hyperplane. Consequently, the set of entropies allowed by all holographic inequalities is called the "holographic entropy cone" [7]. Further following the holographic nomenclature, we will refer to weights of cuts as "areas."

The simplest holographic inequality, known as the monogamy of mutual information [8], is

$$S_{AB} + S_{BC} + S_{CA} \geq S_A + S_B + S_C + S_{ABC}. \qquad (1)$$

Here A, B, C are disjoint subsystems and S_X are their entanglement entropies. Union signs for disjoint regions are implied, for example $AB \equiv A \cup B$. Other than (1), currently known holographic entropy inequalities include one single-parameter infinite family (5) [7] and 378 isolated inequalities [9–11]. However, research thus far has revealed only limited insight into structural patterns or principles, which undergird these constraints [12–23].

Results and relevance. In this work we formulate and prove two new infinite families of holographic entropy inequalities, one indexed by a pair of odd integers and another indexed by one arbitrary integer. These new inequalities prove a prior conjecture, which was motivated by unitary models of black hole evaporation [19]. They also exhibit intriguing connections with diverse corners of theoretical physics, from gravity to quantum information to condensed matter theory, which suggest novel relations among those lines of research. Specific topics of relevance include the following:

(1) Randomness of quantum states. Given a state prepared as a tensor network at large bond dimension, how can we detect that the tensors were not random? A violation of our inequalities is a sufficient condition [2]. That is, the inequalities detect atypical states, independent of network architecture.
(2) A novel role of topology in error correcting codes. The basic rationale for the inequalities is that their violations are prevented by phase transitions. Such transitions are understood in terms of erasure correction [24,25]. Because our inequalities work for topological reasons, they indicate a novel topological aspect of erasure correcting codes such as [26].
(3) Spin models. The proof of the inequalities is strongly reminiscent of the toric code. We elaborate on this at the end of the paper.

(4) Graph theory. Our results are of independent interest there, especially the proof of inequality (17). To our knowledge, they have not appeared in mathematical literature.

This list highlights nonholographic applications. Within holographic duality, the inequalities reveal a previously unappreciated, topological consequence of entanglement wedge nesting [27], which is manifested by a tessellation of a two-dimensional manifold. We also discuss the inequalities' relation to black holes and differential entropy.

Setup and notation. Consider a composite system with $m+n$ constituents, which are called A_i ($1 \leq i \leq m$) and B_j ($1 \leq j \leq n$). The indices on A_i (respectively, B_j) are understood modulo m (respectively, modulo n), for example $i = m+1 \equiv 1$. We assume that this $(m+n)$-partite system is in a pure state; this is equivalent to studying arbitrary states with $m+n-1$ constituents.

Our inequalities are expressed in terms of unions of consecutive A- and B-type regions:

$$A_i^{(k)} = A_i A_{i+1} \ldots A_{i+k-1} \tag{2}$$

and likewise for $B_j^{(l)}$. When m and n are both odd, it is useful to shorthand a special case of this notation, which involves largest consecutive minorities and smallest consecutive majorities of A and B regions:

$$A_i^{\pm} \equiv A_i^{((m\pm1)/2)} \quad \text{and} \quad B_j^{\pm} \equiv B_j^{((n\pm1)/2)}. \tag{3}$$

Throughout the paper, we write the inequalities in the form "lhs $\geq$ rhs" with only positive coefficients.

New inequalities. We prove two new infinite families of holographic inequalities:

(1) Toric inequalities are defined for m and n, which are both odd. They take the following form:

$$\sum_{i=1}^{m}\sum_{j=1}^{n} S_{A_i^+ B_j^-} \geq \sum_{i=1}^{m}\sum_{j=1}^{n} S_{A_i^- B_j^-} + S_{A_1A_2\ldots A_m} \tag{4}$$

The toric character of (4) is related to the symmetry $\mathbb{Z}_m \times \mathbb{Z}_n$, which rotates the A and B regions. [The full symmetry group of (4) is in fact $D_m \times D_n$.]

This family subsumes the dihedral inequalities [7]

$$\sum_{i=1}^{m} S_{A_i^+} \geq \sum_{i=1}^{m} S_{A_i^-} + S_{A_1A_2\ldots A_m} \tag{5}$$

by setting $n=1$ because $B_j^{(0)} = \varnothing$. Inequalities (4) also subsume two other previously known inequalities [9,10]; see Supplemental Material [28].

(2) $\mathbb{RP}^2$ inequalities are indexed by $m = n$:

$$\frac{1}{2}\sum_{i,j=1}^{m}\left(S_{A_i^{(j)}B_{i+j-1}^{(m-j)}} + S_{A_i^{(j)}B_{i+j}^{(m-j)}}\right) \geq \sum_{i,j=1}^{m} S_{A_i^{(j-1)}B_{i+j-1}^{(m-j)}} + S_{A_1A_2\ldots A_m}. \tag{6}$$

We explain momentarily how (6) relates to the projective plane. These inequalities are invariant under D_{2m}, which acts on the regions $B_1, A_1, B_2, A_2 \ldots B_m, A_m$, in this order, like it does on vertices of a regular $(2m)$-gon.

Family (6) includes monogamy of mutual information (1) and one other previously known inequality [9] as special cases ($m = 2$, 3).

We sketch a proof of (4) and (6) in the main text and fill in details in the Supplemental Material [28]. Reference [30] showed that inequalities (4) and (6) are maximally tight, i.e. they are facets of the holographic entropy cone.

Entanglement wedge nesting (EWN). Schematically, each holographic inequality states the following: For any set of minimal cuts that realize the lhs terms, there exist some cuts for the rhs terms with a smaller or equal combined area. With this characterization of the problem, we should expect that facts and theorems about minimal cuts are likely to inform the structure and proofs of holographic entropy inequalities. This paper exploits one such fact, known as the EWN theorem [27].

The theorem says that if two composite regions X, Y are in either of these two relationships

$$X \subset Y \quad \text{or} \quad X \subset \bar{Y}, \tag{7}$$

then the minimal cuts for S_X and S_Y can meet but cannot intersect; see Fig. 1. In the AdS/CFT correspondence, subregion duality [31,32] states that the largest bulk region reconstructible with access to boundary subsystem X—the entanglement wedge of X—is enclosed by X and the minimal cut for X. This statement logically requires the EWN theorem or else extra access to $Y \backslash X$ would limit one's ability to reconstruct the bulk.

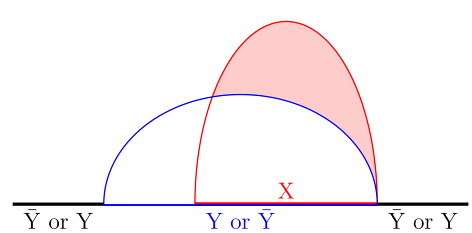

FIG. 1. Intersecting minimal cuts, which are forbidden by the entanglement wedge nesting theorem.

As we explain below, inequalities (4) and (6)—and the crux of their proof—concern structural constraints on minimal cuts, which are induced by entanglement wedge nesting and which arise for topological reasons.

Geometric organization. We propose a graphical way to organize terms of holographic inequalities, which is based on entanglement wedge nesting. We represent lhs terms as facets and rhs terms as vertices of a graph. Facets are defined with respect to an embedding on a two-dimensional surface, which we discuss momentarily. The organizing rule for the graph is that a vertex (rhs term) is incident to a facet (a lhs term) if and only if they satisfy a nesting relationship (7).

A priori, it is not guaranteed that applying this rule to a holographic inequality will produce a sensible graph, which can be embedded on a two-dimensional manifold. Yet it turns out to work perfectly for inequalities (4) and (6), with illuminating consequences.

The result of applying this graphical rule to inequalities (4) is shown in the upper panel of Fig. 2. It is a rhombus with diagonals spanning m and n squares and with opposite sides identified—a tessellation of a torus. The special term $S_{A_1A_2\ldots A_m}$ is left out of the graph because it is not in a nesting relationship with other terms.

For inequalities (6), the result is shown in the lower panel of Fig. 2. *A priori*, the special rhs term $S_{A_1A_2\ldots A_m}$ could be canceled out because the lhs contains m copies of the same. Taking inspiration from the toric inequalities, we do not

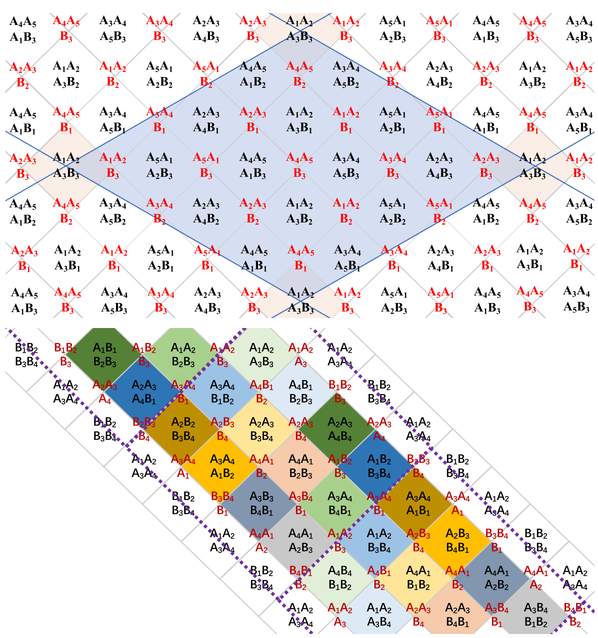

FIG. 2. Graphical representations of a toric $[(m,n)=(5,3)$; upper panel] and an $\mathbb{RP}^2$ inequality ($m=4$; lower panel). Diamonds of same color are equivalent. We highlight fundamental domains of periodic identifications.

cancel it but leave it out of the graph. This produces an $m\times m$ array of squares with one reflected periodic identification—a tessellation of the Möbius strip. The identification involves complementary regions with equal entropies, for example:

$$S_{A_i^{(j)}B_{i+j}^{(m-j)}} = S_{A_{i+j}^{(m-j)}B_i^{(j)}}. \tag{8}$$

The boundary of this Möbius strip consists of m identical terms $S_{A_1A_2\ldots A_m} = S_{B_1B_2\ldots B_m}$. If we treat them all as one facet, then we effectively glue the Möbius strip to a disk, which produces the projective plane $\mathbb{RP}^2$.

Sketch of proof of inequalities. Reference [7] reduced the task of proving holographic entropy inequalities to finding maps $x \to f(x)\colon \{0,1\}^l \to \{0,1\}^r$, which satisfy

$$|x-x'|_1 \geq |f(x)-f(x')|_1 \qquad x,x' \in \{0,1\}^l \tag{9}$$

as well as certain inequality-specific boundary conditions. Here l and r refer to the numbers of terms on the lhs and rhs of the inequality, accounting for multiplicity, such that component bits of $x\in\{0,1\}^l$ and $f(x)\in\{0,1\}^r$ are associated to individual terms of the inequality. The rationale for and details of this method of proof are reviewed in the Supplemental Material [28].

The contraction that proves inequalities (4) is defined as follows. The proof of (6) is similar in spirit; see Supplemental Material [28]. Since our graphical scheme represents lhs terms as facets in a square tiling, every $x\in\{0,1\}^l$ is an assignment of 0s and 1s to squares. The contraction $f(x)\in\{0,1\}^r$ assigns 0 or 1 to every vertex in the tiling and to the special term $S_{A_1A_2\ldots A_m}$ not present in the tiling. To express $f(x)$, define a graph $\Gamma(x)$ by drawing a horizontal/vertical pair of line segments on every square that carries a 0/1, as shown in Fig. 3. Because every node of $\Gamma(x)$—that is, every edge in the tiling—is connected to two other nodes, $\Gamma(x)$ is composed of nonintersecting loops. Therefore, $\Gamma(x)$ partitions the torus into components. Map f assigns 1 to one special vertex (say, bottommost and

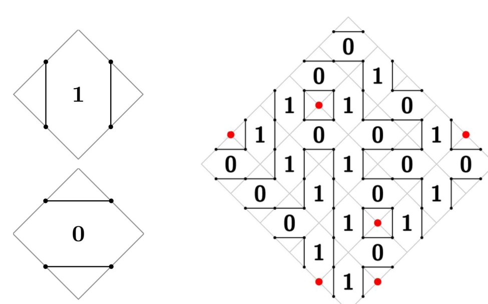

FIG. 3. Rules for drawing graphs $\Gamma(x)$ and one such graph, which arises in proving the (5,5) toric inequality. Tiling vertices, which are mapped to 1 under $f(x)$, are highlighted.

rightmost) in every component, which does not wrap a nontrivial cycle of the torus. To all other vertices f assigns 0.

Finally, the value of f in the last bit (on the special rhs term $S_{A_1A_2\ldots A_m}$) is set so that $|x|_1 \equiv |f(x)|_1 \pmod 2$. This condition turns out to equivalently characterize the torus cycle, which is wrapped by the noncontractible loop(s) in $\Gamma(x)$.

For details, and to confirm that f is indeed a contraction, see the Supplemental Material [28]. Here we wish to convey that the spatial organization of terms as facets and vertices on a manifold is indispensable for proving the inequalities. The logic of the proof indicates that inequalities (4) and (6) are topological statements undergirded by entanglement wedge nesting.

Inequalities versus strong subadditivity. Consider one edge of the tiling in Fig. 2. Let the two facets incident to the edge be S_X and $S_{\bar{V}}$. An inspection of the inequalities reveals that the vertices incident to the edge are $S_{\overline{X\cup V}}$ and $S_{X\cap V}$. For example, in inequalities (4), the edge that separates the facets with

$$X = A_i^+ B_j^- \quad \text{and} \quad \bar{V} = A^+_{i+(m-1)/2} B^-_{j+(n+1)/2} \tag{10}$$

has end points at

$$\overline{X\cup V} = A^-_{i+(m+1)/2} B^-_{j+(n+1)/2} \quad \text{and} \quad X\cap V = A_i^- B_j^-.$$

The same observation holds in the graph of (6).

If we now collect the four terms that are associated with one edge, then we obtain a nonnegative [33] quantity called conditional mutual information:

$$\mathrm{CMI}_{\mathrm{edge}} \coloneqq S_X + S_V - S_{X\cap V} - S_{X\cup V}. \tag{11}$$

We have used the fact that we are working with pure states so complementary regions have equal entropies.

After adding up contributions from various edges, and correcting for a double-counting of terms, we discover that inequalities (4), (6) can be written in the simple form:

$$\frac{1}{2}\sum{}' \mathrm{CMI}_{\mathrm{edges}} \geq S_{A_1A_2\ldots A_m}. \tag{12}$$

In toric inequalities, the $\sum'$ runs over either set of parallel edges. In the $\mathbb{RP}^2$ inequalities we sum over edges, which run parallel to the boundary of the Möbius strip in Fig. 2. Rewriting (12) presents the inequalities as a collective improvement on strong subadditivity.

Continuum limit. The regular structure of the inequalities allows us to take a continuum limit $m, n \to \infty$. The idea is to keep the union of all A- and B-type regions fixed, but subdivide it into a growing number of A_is and B_js. Due to the cyclic symmetries that rotate the A and B regions, it is easiest to visualize a special case: an entangled state of two $(1+1)$-dimensional holographic conformal field theories (CFT_2) living on circles, which are subdivided into intervals A_i and B_j. Holographically, this setup describes a $(2+1)$-dimensional, two-sided black hole with entropy $S_{\mathrm{BH}} = S_{A_1A_2\ldots A_m}$.

In these settings, studying the continuum limit of holographic inequalities has a useful precedent. Taking $m \to \infty$ in subfamily (5) of the toric inequalities gives

$$S_{\mathrm{diff}} = \oint dv \left.\frac{\partial S(u,v)}{\partial v}\right|_{u=u(v)} \geq S_{A_1A_2\ldots A_m} = S_{\mathrm{BH}}, \tag{13}$$

where $S(u,v)$ is the entanglement entropy of interval (u,v). In expression (13), we traded the discrete label i in A_i^+ for a continuous variable v using $A_i^+ \coloneqq (u(v), v)$, so that the function $u(v)$ implicitly encodes the sizes of intervals A_i^+. Quantity S_{diff}, called differential entropy [34,35], computes the length of the bulk curve whose tangents subtend boundary intervals $(u(v), v)$. Inequality (13) is manifestly true because such a curve necessarily wraps around the black hole horizon.

For a similar limit of inequalities (4), let $A_i^+ = (u_A, v_A(u_A))$ and $B_j^- = (u_B(v_B), v_B)$. Observing that in the continuum limit quantity $\mathrm{CMI}_{\mathrm{edge}}$ becomes a second partial derivative of entropy, we find

$$-\frac{1}{2}\oiint du_A dv_B \frac{\partial^2 S(u_A, v_A; u_B, v_B)}{\partial u_A \partial v_B} \geq S_{\mathrm{BH}}. \tag{14}$$

The integral in (14) admits many bulk interpretations, depending on the phases of $S(u_A, v_A; u_B, v_B)$. Its behaviors—as well as the continuum limit of inequalities (6)—will be studied in a separate publication [36].

To give a flavor of the bulk interpretation of (14), we consider one illustrative case. Assume that the Ryu-Takayanagi surfaces for $A_i^\pm B_j^-$ do not wrap or cross the horizon; this can be easily arranged by choosing a shockwave geometry [37] with a large horizon. Then the terms in (4) can only be in one of two phases:

$$S_{A_i^\pm B_j^-} = (S_{A_i^\pm} + S_{B_j^-}) \quad \text{or} \quad (S_{A^\mp_{i+(m\pm1)/2}} + S_{B^+_{j+(n-1)/2}}).$$

Suppose B_n is much larger than all the other regions, so that the phase of $S_{A_i^\pm B_j^-}$ is determined solely by whether or not $B_n \subset B_j^-$. Substituting in Eqs. (10) and (11), we see that the only nonvanishing terms in (12) arise from $X = A_i^+ B^-_{(n+1)/2}$ and $\bar{V} = A^+_{i+(m-1)/2} B_1^-$ and evaluate to

$$\mathrm{CMI}_{\mathrm{edge}} = (S_{A_i^+} - S_{A_i^-}) + (S_{A^+_{i+(m-1)/2}} - S_{A^-_{i+(m+1)/2}}) \xrightarrow{\text{continuum}} dv_A \frac{\partial S(u_A, v_A)}{\partial v_A} - du_A \frac{\partial S(u_A, v_A)}{\partial u_A}. \quad (15)$$

Replacing $\frac{1}{2}\sum' \to \frac{1}{2}\oint$ and integrating by parts, we again find (13). Thus, toric inequalities also reproduce the geometric fact "differential entropy ≥ black hole entropy."

Significance for the holographic entropy cone. In searching for order among holographic inequalities, two of us previously conjectured a pattern [19] (see also [20]). Take any valid inequality and apply to it the permutation group acting on region labels. Adding up all permutation images gives a weaker inequality, which involves only averages of p-partite entropies, denoted S^p. For example, averaging monogamy (1) in this way gives

$$(S_{AB} + S_{BC} + S_{CA}) \geq (S_A + S_B + S_C) + S_{ABC} \to 3S^2 \geq 3S^1 + S^3. \quad (16)$$

We conjectured that for every p there exists a valid holographic inequality on $2p - 1$ or more regions which, after averaging, gives

$$2S^p/p \geq S^{p-1}/(p-1) + S^{p+1}/(p+1). \quad (17)$$

If valid, inequalities (17) cannot be improved. That is, every valid holographic inequality averages to a convex combination of (17). This is because so-called extreme rays—values of S^p that simultaneously saturate all but one inequality (17)—have known realizations as tensor networks and holographic geometries, so any improvement over (17) is necessarily wrong. These extreme rays correspond rigorously to stages of evaporation of an old black hole—a fact that motivated our conjecture.

Each family presented in this paper independently proves the conjecture. Indeed, toric inequalities with $m = n$ and $m = n + 2$ average to (17) with $p = (m + n)/2$ while the $\mathbb{RP}^2$ inequalities average to (17) with $p = m$.

At present, we know 375 holographic inequalities, which are not part of families (4), (6). It will be interesting to see whether they too are associated with two-dimensional manifolds under our EWN-based graphical scheme. We have not yet checked this because 373 of them were announced only recently [11]. Encouragingly, the answer is affirmative for one of the "older" inequalities: it defines a polytope with the topology of the four-cross-cap surface; see the Supplemental Material [28].

Applications outside holographic duality. In holographic error correcting codes such as [26], the maximal number of degrees of freedom protected against erasure of $\bar{A}$ is $(\log \dim \mathcal{H}_A) - S_A$ [24]. Inequalities (4) set an upper bound on $S_{A_1 A_2 \ldots A_m}$, which in turn bounds from below the size of the largest code subspace protected against erasing $B_1 B_2 \ldots B_n$. We stress that the bound arises due to the toroidal topology of the abstract polytope, which is formally assembled from regions $A_i^{\pm} B_j^-$.

The topological origin of this bound may be further illuminated by a comparison with the toric code [38]. In the latter, logical qubits are represented by noncontractible loops in the loop gas picture of the wave function. Our proof of the inequalities is in many respects reminiscent of the construction of the ground state wave function of the toric code. Specifically, the proof relates $S_{A_1 A_2 \ldots A_m}$ to loops in graph $\Gamma(x)$ which—like the carriers of logical qubits in the toric code—wrap noncontractible cycles of the torus. We hope to recast our proof as constructing a wave function of a variant of the toric code, whose logical qubits directly manifest the bound on $S_{A_1 A_2 \ldots A_m}$.

Acknowledgments. We thank for useful discussions Bowen Chen, Sergio Hernández-Cuenca, Ricardo Espíndola, Matthew Headrick, Veronika Hubeny, Xiao-Liang Qi, Yunfei Wang, Dachen Zhang as well as participants of the "Quantum Information, Quantum Matter and Quantum Gravity" workshop (YITP-T-23-01) held at YITP, Kyoto University (2023), where this work was completed. Y. W. acknowledges support from the Shuimu Tsinghua Scholar Program of Tsinghua University. This research was supported by an NSFC Grant No. 12042505, a BJNSF grant under the Gao Cengci Rencai Zizhu program, and a Dushi Zhuanxiang Fellowship. B. C. dedicates this paper to Bayu Miłosz Czech in celebration of his seventh birthday.

[1] J. M. Maldacena, The large N limit of superconformal field theories and supergravity, Adv. Theor. Math. Phys. **2**, 231 (1998).

[2] P. Hayden, S. Nezami, X. L. Qi, N. Thomas, M. Walter, and Z. Yang, Holographic duality from random tensor networks, J. High Energy Phys. 11 (2016) 009.

[3] S. Ryu and T. Takayanagi, Holographic derivation of entanglement entropy from AdS/CFT, Phys. Rev. Lett. **96**, 181602 (2006).

[4] S. Ryu and T. Takayanagi, Aspects of holographic entanglement entropy, J. High Energy Phys. 08 (2006) 045.

[5] V. E. Hubeny, M. Rangamani, and T. Takayanagi, A covariant holographic entanglement entropy proposal, J. High Energy Phys. 07 (2007) 062.
[6] N. Engelhardt and A. C. Wall, Quantum extremal surfaces: Holographic entanglement entropy beyond the classical regime, J. High Energy Phys. 01 (2015) 073.
[7] N. Bao, S. Nezami, H. Ooguri, B. Stoica, J. Sully, and M. Walter, The holographic entropy cone, J. High Energy Phys. 09 (2015) 130.
[8] P. Hayden, M. Headrick, and A. Maloney, Holographic mutual information is monogamous, Phys. Rev. D **87**, 046003 (2013).
[9] S. Hernández-Cuenca, Holographic entropy cone for five regions, Phys. Rev. D **100**, 026004 (2019).
[10] B. Czech and Y. Wang, A holographic inequality for $N = 7$ regions, J. High Energy Phys. 01 (2023) 101.
[11] S. Hernández-Cuenca, V. E. Hubeny, and F. Jia, Holographic entropy inequalities and multipartite entanglement, arXiv:2309.06296.
[12] S. X. Cui, P. Hayden, T. He, M. Headrick, B. Stoica, and M. Walter, Bit threads and holographic monogamy, Commun. Math. Phys. **376**, 609 (2019).
[13] V. E. Hubeny, M. Rangamani, and M. Rota, Holographic entropy relations, Fortschr. Phys. **66**, 1800067 (2018).
[14] V. E. Hubeny, M. Rangamani, and M. Rota, The holographic entropy arrangement, Fortschr. Phys. **67**, 1900011 (2019).
[15] B. Czech and X. Dong, Holographic entropy cone with time dependence in two dimensions, J. High Energy Phys. 10 (2019) 177.
[16] T. He, M. Headrick, and V. E. Hubeny, Holographic entropy relations repackaged, J. High Energy Phys. 10 (2019) 118.
[17] T. He, V. E. Hubeny, and M. Rangamani, Superbalance of holographic entropy inequalities, J. High Energy Phys. 07 (2020) 245.
[18] C. Akers, S. Hernández-Cuenca, and P. Rath, Quantum extremal surfaces and the holographic entropy cone, J. High Energy Phys. 11 (2021) 177.
[19] B. Czech and S. Shuai, Holographic cone of average entropies, Commun. Phys. **5**, 244 (2022).
[20] M. Fadel and S. Hernández-Cuenca, Symmetrized holographic entropy cone, Phys. Rev. D **105**, 086008 (2022).
[21] S. Hernández-Cuenca, V. E. Hubeny, and M. Rota, The holographic entropy cone from marginal independence, J. High Energy Phys. 09 (2022) 190.
[22] T. He, V. E. Hubeny, and M. Rota, On the relation between the subadditivity cone and the quantum entropy cone, J. High Energy Phys. 08 (2023) 018.
[23] T. He, V. E. Hubeny, and M. Rota, A gap between holographic and quantum mechanical extreme rays of the subadditivity cone, Phys. Rev. D **109**, L041901 (2024).
[24] A. Almheiri, X. Dong, and D. Harlow, Bulk locality and quantum error correction in AdS/CFT, J. High Energy Phys. 04 (2015) 163.
[25] D. Harlow, The Ryu–Takayanagi formula from quantum error correction, Commun. Math. Phys. **354**, 865 (2017).
[26] F. Pastawski, B. Yoshida, D. Harlow, and J. Preskill, Holographic quantum error-correcting codes: Toy models for the bulk/boundary correspondence, J. High Energy Phys. 06 (2015) 149.
[27] C. Akers, J. Koeller, S. Leichenauer, and A. Levine, Geometric constraints from subregion duality beyond the classical regime, arXiv:1610.08968.
[28] See Supplemental Material at http://link.aps.org/supplemental/10.1103/PhysRevD.109.L101903; it contains three parts. Part A reviews previously known holographic entropy inequalities, which appear as special cases in the two families presented in this paper. We also discuss one other inequality, which our graphical scheme maps to the four-cross-cap surface. Parts B and C prove inequalities (4) and (6). Supplemental Material cites Ref. [29], which is not cited in the main text.
[29] R. P. Stanley, *Catalan Numbers* (Cambridge University Press, Cambridge, England, 2015).
[30] B. Czech, Y. Liu, and B. Yu, Two infinite families of facets of the holographic entropy cone, arXiv:2401.13029.
[31] B. Czech, J. L. Karczmarek, F. Nogueira, and M. Van Raamsdonk, The gravity dual of a density matrix, Classical Quantum Gravity **29**, 155009 (2012).
[32] X. Dong, D. Harlow, and A. C. Wall, Reconstruction of bulk operators within the entanglement wedge in gauge-gravity duality, Phys. Rev. Lett. **117**, 021601 (2016).
[33] E. H. Lieb and M. B. Ruskai, Proof of the strong subadditivity of quantum-mechanical entropy, J. Math. Phys. (N.Y.) **14**, 1938 (1973).
[34] V. Balasubramanian, B. D. Chowdhury, B. Czech, J. de Boer, and M. P. Heller, Bulk curves from boundary data in holography, Phys. Rev. D **89**, 086004 (2014).
[35] M. Headrick, R. C. Myers, and J. Wien, Holographic holes and differential entropy, J. High Energy Phys. 10 (2014) 149.
[36] B. Chen, B. Czech, R. Espíndola, and Dachen Zhang (to be published).
[37] S. H. Shenker and D. Stanford, Multiple shocks, J. High Energy Phys. 12 (2014) 046.
[38] A. Kitaev, Anyons in an exactly solved model and beyond, Ann. Phys. (Amsterdam) **321**, 2 (2006).